SLAC–PUB–4795
June 1989
(I)

DEVELOPMENT AND CONSTRUCTION OF THE SLD ČERENKOV RING IMAGING DETECTOR*

D. ASTON,[a] A. BEAN,[c] T. BIENZ,[a] F. BIRD,[a,†] D. CALDWELL,[c]
M. CAVALLI–SFORZA,[d] P. COYLE,[d] D. COYNE,[d] S. DASU,[a] W. DUNWOODIE,[a]
G. HALLEWELL,[a,‡] K. HASEGAWA,[g] J. HUBER,[c] P. JACQUES,[f] R. A. JOHNSON,[e]
H. KAWAHARA,[a] P. KORFF,[a] Y. KWON,[a] D. LEITH,[a] A. LU,[c] J. MARTINEZ,[e] L. MATHYS,[c]
S. MCHUGH,[c] B. MEADOWS,[e] M. NUSSBAUM,[e] R. MORRISON,[c] R. PLANO,[f] B. RATCLIFF,[a]
P. RENSING,[a] D. SCHULTZ,[a] S. SHAPIRO,[a] A. SHOUP,[e] C. SIMOPOULOS,[a] E. SOLODOV,[a,§]
P. STAMER,[f] I. STOCKDALE,[e] N. TOGE,[a] J. VA'VRA,[a] D. A. WILLIAMS,[d] S. WILLIAMS,[a]
M. WITHERELL,[c] R. J. WILSON,[b] J. S. WHITAKER,[b] S. YELLIN,[c] H. YUTA[g]

[a] *Stanford Linear Accelerator Center, Stanford University, Stanford, CA 94309*
[b] *Boston University, Dept. of Physics, Boston, MA 02215*
[c] *University of California, Dept. of Physics, Santa Barbara, CA 93106*
[d] *Santa Cruz Institute for Particle Physics, University of California, Santa Cruz, CA 95064*
[e] *University of Cincinnati, Dept. of Physics, Cincinnati, OH 45221*
[f] *Rutgers University, Dept. of Physics, New Brunswick, NJ 08903*
[g] *Tohoku University, Dept. of Physics, Aramaki, Sendai 980, Japan*
[h] *Yale University, Dept. of Physics, New Haven, CT 06511*

Presented by G. Hallewell at the International Wire Chamber Conference, Vienna, Austria, February 13–17, 1989.

---

* Work supported by the Department of Energy, Department of Energy contracts DE-AC03–76SF00515 and DE–AT03–79ER70023, and by the National Science Foundation under grants PHY85–12145 and PHY85–13808.

† Present Address: EP Division, CERN, CH–1211, Geneva 23, Switzerland.
§ Permanent Address: Institute of Nuclear Physics, Novosibirsk, 630090, USSR.
‡ Speaker.

ABSTRACT

We report on the development and construction of the Čerenkov Ring Imaging Detector (CRID) for the SLD experiment at the SLAC linear collider. In particular, we outline recent progress in the construction, and results from testing the first components of the barrel CRID, including the drift boxes, liquid radiator trays and mirror system. We also review progress in the construction of the barrel CRID gas radiator vessel, the liquid radiator recirculator system, and the electronic readout system. The development of a comprehensive monitor and control system—upon which the stable operation and physics efficacy of the CRID depend—is also described.

1. INTRODUCTION

A large Čerenkov Ring Imaging Detector (CRID)[1,2] is currently under construction for the SLD experiment at the SLAC Linear Collider (SLC), and will provide almost complete particle identification over 90% of the solid angle at the SLC, using barrel and endcap segments [Figs. 1(a) and 1(b)]. By making use of both liquid[(a)] and gaseous[(b)] radiators, $\pi/K/p$ separation will be possible up to about 30 GeV/c, and e/π separation up to about 6 GeV/c.

Čerenkov photons entering drift boxes with quartz windows will ionize a drift gas mixture containing about 0.1% of TMAE[(c)] the resulting photoelectrons, which drift up to 1.25 m in a uniform electric field, will be detected and localized using charge division along 7 μm carbon sense fibers.[3–5]

From our test results,[3] we expect to observe Čerenkov rings containing a maximum of 14 photoelectrons from the passage of $\beta = 1$ particles through the 45 cm gas radiator, and ≥ 25 photoelectrons per ring from the 1-cm-thick liquid radiator at normal incidence.

As an example of the particle identification capability, π/K separation of $>10\sigma$ has been achieved in an 11 GeV/c test beam using only the gas radiator.[3]

(*a*) C_6F_{14}: [perfluoro-n-hexane]; n = 1.227 at $\lambda = 200$ nm; PP1 Grade, I. S. C. Co., Bristol, UK.
(*b*) C_5F_{12}: [perfluoro-n-pentane]; n = 1.0017 at $\lambda = 200$ nm; PP50 Grade, I. S. C. Co., Bristol, UK.
(*c*) Tetrakis(Dimethylamino)Ethylene: $E_i = 5.3$ eV .

2. DEVELOPMENT AND CONSTRUCTION OF THE BARREL CRID

2.1 Structure of the Barrel CRID Vessel

The mechanical construction of this vessel is now well advanced, with all the major structural components in place. The major internal components—the 40 C_6F_{14} liquid radiator trays, drift boxes and mirror arrays—will be contained, together with the C_5F_{12} radiator gas, within a cylindrical shell with inner and outer radii 102 and 177 cm, situated between the central drift chamber (CDC) and liquid argon calorimeter (LAC) of the SLD [Fig. 1(b)].

The inner wall is constructed from five composite panels of 8-mm phenolic-impregnated paper honeycomb[(d)] laminated between 0.5 mm aluminum sheets, while the outer wall is formed by the inner surface of the LAC vacuum cylinder, which has a wall thickness of 32 mm.

The other major fixed components of the CRID vessel are a grid of axial locking rails which accept the 40 externally prealigned mirror arrays (see Sec. 2.4), and a central high voltage distribution board, delivering a potential of 50–60 kV to the inboard ends of the 40 drift boxes (for a typical drift field of 400 V/cm). This potential is degraded to ground over a distance of about 65 cm to the CRID outer cylinder by resistive pitches defined between 25 concentric conducting traces etched on the distribution board. Over the 10-cm distance to the CRID inner cylinder, the external potentials are controlled with the aid of thick wire external field cages on the individual drift boxes [Fig. 1(a), Sec. 2.2].

Since accurate control of the CRID operating temperature is essential in order to maintain the correct concentration of TMAE in the drift gas, and to prevent the condensation of the C_5F_{12} radiator gas—which occurs at about 30°C at atmospheric pressure—the vessel surfaces are populated with an array of Kapton-insulated heater pads and temperature sensors.[(e)] Power will be divided between "distributed" circuits

(*d*) Hexcell Corp., Dublin, CA 94566.
(*e*) AD590: Analog Devices, Inc., Norwood MA 02062.

whose pads are scattered in a regular geometric pattern over the whole surface of the vessel to provide uniform background heat, and "local" circuits whose pads are grouped close together to provide local trim. Approximately 200 heater circuits will be used in conjunction with about 300 temperature sensors to maintain the vessel at a safe, uniform temperature of about 40°C, and will provide a high level of redundancy.

The CAMAC-based temperature control system activates heater circuits on the basis of temperatures monitored by nearby sensors. A software database stores the required temperature setpoints and the geometric correlation between sensor positions and heater pad circuits. In the event of a heater circuit failure, the software automatically compensates by switching control to remaining circuits and increasing their "on-time" duty cycle. A failed temperature sensor is automatically dropped from the active list on which heater operations are performed.

2.2 Performance Evaluation of the Barrel CRID Drift Boxes

Production of the 40 drift boxes for the barrel CRID is proceeding on an assembly-line basis with rigorous quality control during all stages of construction. Six boxes are currently under construction, and two completed boxes are undergoing performance evaluation. Since many of the details of construction have been discussed elsewhere,[2] this report is confined to those directly relevant to drift box performance.

To ensure a uniform electric field in the drift boxes, and to shield drifting electrons from the disturbing effects of nearby grounds—in particular the presence of the inner wall of the CRID vessel about 10 cm away—external field cages are fitted [Fig. 1(a)], and graded-potential conductors are attached to both sides of the quartz windows. The windows taper apart so that electrons drift away from the quartz surfaces and the effects of transverse diffusion and local drift field irregularities are reduced. An asymmetric taper[2] is used to help align the electron trajectories with the SLD magnetic field, which has a moderate radial component.

Electrons are efficiently focused to the 7-μm-diam carbon anode fibers by a series of voltage-graded conducting grids— described in more detail in a separate contribution to this conference.[8] These also serve, together with the scalloped cathode block to reduce "photon feedback" from the conversion of secondary UV photons liberated in the avalanches at the sense wires. Gating electrodes are also provided to inhibit the entry of out-of-time electrons into the detection volume, or positive ions into the drift volume. The drift field-defining and focusing array conductors are photochemically etched from single sheets of beryllium/copper alloy.

The only materials used in drift box manufacture are those known to be compatible with TMAE,[9] and which do not outgas electronegative or UV-absorbing products. Despite the choice of "non-FR4" G10 (epoxy-glass laminate using nonbrominated epoxies), we have found that the lifetime of electrons in the drift boxes is adversely affected[8] unless the G10 is coated with either DP190[(f)] or a combination of EPON826[(g)] and VERSAMID 140[(h)] epoxies. Of particular concern is the outgassing from lamination epoxies under the drift field defining printed circuit traces on the side walls of the drift boxes. Painting between the traces is very difficult, and painting over the copper surface can distort the field if the resistivity of the epoxy is too high to allow the surface charge to quickly leak away. A three-part, low surface and volume resistivity epoxy[(i)] was found to react with TMAE over long periods. Although DP190 has a higher resistivity at room temperature,[10] this drops by a factor of 100 as the CRID operating point of 40°C is approached (Fig. 2). With a DP190 coating, electron lifetimes—measured indirectly with an ionization chamber[8] (Fig. 4) — >120 μs have been seen in methane/TMAE, corresponding to an attenuation length of about 10 m.

The UV transparency of all quartz sheets is measured in a vacuum test station large enough to allow a UV beam to scan over the whole 125 × 30 cm surface of a drift box, or liquid radiator tray, window. Figure 3(a) is an example of the measured transmission in an acceptable sheet[11] ($\geq$85% for $\lambda \geq$175 nm). The effects of insufficient surface polish or impurities in the bulk material in two rejected sheets are shown in Figs. 3(b) and 3(c).

(*f*) 3–M Co.
(*g*) Shell Co.
(*h*) Henkel Co.
(*i*) CIBA–GEIGY 508, 6005, 956.

Most of the production drift boxes will be put through a program of tests in the apparatus of Fig. 4. The drift gas[(j)] is ionized at several points with either a UV laser on an X–Y stage, or via the fixed fiducial matrix of 19 UV-transmitting optical fibers integral to each drift box. Distortions in the trajectories of drifting electrons will be inferred by comparing the reconstructed light spots with their known positions. An extensive study of electron drift distortions is currently in progress in the first of our production drift boxes.

2.3 Construction of the Barrel CRID Liquid Radiator Trays

Each drift box will be illuminated by Čerenkov light produced in 10 mm of C_6F_{14} held within a liquid radiator tray [Figs. 1(b) and 5(b)]. Trays will be installed in 20 distinct azimuthal orientations and will operate at hydrostatic pressures varying in the range $0.02 - 0.06$ Kg cm^{-2} .

Before beginning a program of tray construction, it has been necessary to fully understand the effects of chemical exposure and the hydrostatic pressure of C_6F_{14} ($\rho = 1.65$ g cm^{-3} at 40°C) upon the materials and adhesives used for tray manufacture. A quartz/G10 joint made with DP190 adhesive has been exposed to C_6F_{14} under pressure at 40°C for ten months with no failure or observable creepage. In a detailed study made in a test tray with a 3.2-mm-thick glass window, tray deflections were measured over a long time period at many points under varying orientations and were found to be elastic as the C_6F_{14} hydrostatic pressure was increased over a wide range [Fig. 5(a)]. There was little evidence of inelastic deformation before the glass window failed, as expected, at a calculated stress of 545 Kg cm^{-2}. These results are encouraging, since glass has a quoted tensile strength only 80% that of quartz, and the breaking stress corresponded to a C_6F_{14} hydrostatic head greater than four times the maximum envisioned operating pressure. Although the production liquid radiator trays are more conservatively built using 4 mm quartz [Fig. 5(b)], the first of four such trays so far completed is being used in a similar long-term structural test.

(j) We are planning to use ethane (C_2H_6) or a methane/ethane (CH_4/C_2H_6) mixture as the drift gas in the barrel CRID drift boxes.

To prevent polarization of the liquid radiator tray quartz windows—and resulting distortion of the trajectories of electrons in the nearby drift boxes—the upper surfaces are equipped with grids of wires which may be grounded to allow any surface charges to leak away [Fig. 5(b)].

The liquid radiator recirculator system is currently under fabrication. C_6F_{14} will circulate under gravity through liquid trays at various levels. At each level the pressure is defined by a local reservoir which provides a small hydrostatic head to drive the liquid through the tray. An overflow into a common manifold limits the head. Each tray has its own return line for monitoring purposes, and its liquid can be switched under computer control into a monitor station measuring water, dissolved oxygen and UV transparency levels. The liquid from all the trays is collected in a low level sump and pumped back to a high level reservoir and purifier[(k)] before being recirculated through the trays.

2.4 Construction of the Barrel CRID Mirror System

Each drift box will accept light from a prealigned array of ten spherical mirrors covering polar angles out to 46°. Five different mirror sizes—all approximately 30 cm × 30 cm, 6-mm-thick with radii of curvature of 95.8 or 101.6 cm are used. Mirror production is proceeding smoothly, and approximately 80 of the 400 mirrors for the barrel CRID have now been completed and tested.

To ensure the high final reflectivity specification of ($\geq$80% at λ = 160 nm and $\geq$85% for λ $\geq$170 nm), and a small contribution from optical distortions to the overall photoelectron reconstruction uncertainty of about 1 mm,[3] the surface finish and sphericity of the mirror substrates must be sufficient to scatter no more than a few per cent of the incident light, and must give an angular reflection error of $\leq$1 mrad. This quality is now routinely achieved in a two-step manufacturing process:[(l)]

(*i*) 6 mm glass blanks are "slumped"(heated and pulled into spherical molds under vacuum);

(*k*) "OXISORB"; Messer Greisheim, West Germany.
(*l*) Mirror substrates manufactured by Lancaster Glass Co., Lancaster, OH 43130.

(*ii*) the contoured blank is ground and polished to produce a substrate with a surface roughness ≤ 3 nm (rms).

The optical distortion from each mirror substrate is measured photographically,[2] and the surface roughness is examined locally, interferometrically with a profilometer.[(m)] Figure 6(a) shows an example of the rms surface roughness measured on one of the substrates. Of approximately 250 production mirror blanks so far examined, only 7% have failed to meet our acceptance criteria.

Acceptable mirror substrates are coated with approximately 80 nm of aluminum and 40 nm of magnesium fluoride under high vacuum.[(n)]

A custom instrument has been constructed to measure the reflectivity of each full size mirror. A UV monochromator with a deuterium lamp directs a narrow beam of light onto the test mirror, which reflects the light into a photomultiplier. The test mirror can be pivoted about its center of curvature, and rotated about its center point, allowing any point on its surface to be illuminated.

We have found that the reflectivities of all of the 80 production mirrors so far completed exceed our specification. Figure 6(b) shows the average reflectivity measured in a sample of 25 mirrors.

3. CRID ENDCAP DEVELOPMENTS

Research and development for the endcap CRID is progressing well, and several important design decisions have been made. The endcap CRID will have the same tenfold azimuthally-symmetric geometry of mechanically separate wedge-shaped sectors as the barrel. Photoelectrons will drift radially outward, perpendicular to the 0.6 T magnetic field of the SLD, in an electric field defined by conductors on the quartz windows, to sense planes located around the circumference.

Although a large number of sectors is desirable to maximize the area covered, the number is limited in practice by the requirement that the sector opening angle be at

(*m*) Applied Magnetics Co., Goleta, CA 93117.
(*n*) Acton Research Corp., Acton, MA 01720.

least twice the Lorentz angle in order for all the ionization produced in a given sector to drift toward the sense plane.

An extensive search has been made[12] for a low Lorentz angle drift gas mixture with good UV transparency and quenching properties, and with sufficient gain for efficient single electron detection. Other necessary properties are a long attenuation length for electron capture to allow efficient drift over long distances, and a small spatial diffusion coefficient to maintain good resolution. Theoretical calculations have indicated that drift mixtures of ethane and carbon dioxide (C_2H_6/CO_2) are well suited to a ten-fold sector geometry for fractional CO_2 concentrations in excess of 10%. Electron lifetimes in 80% C_2H_6/20% CO_2 have been measured to be in excess of 190 μs.

Figure 7 shows the single electron pulse height spectra measured on 7 μm carbon at a variety of cathode voltages for a gas mixture of 80% C_2H_6/20% CO_2.

The small Lorentz angle in C_2H_6/CO_2 also simplifies the transfer of electrons from the drift region to the detector region. The electron focusing and optical blinding geometry of the barrel CRID[2,6] is impractical in the endcap CRID, where the magnetic field would divert electrons onto trajectories that terminate prematurely on the focusing grid. Several compact structures are under consideration, which are efficient not only during normal operation in the magnetic field, but also when the field is turned off. This feature will greatly simplify testing procedures. Figure 8 is a simulation of electron focussing in a mixture of 80% C_2H_6/20% CO_2 (Lorentz angle = $10°$) in one such structure.

4. THE CRID READOUT SYSTEM

We have made significant progress in the development and implementation of the CRID readout system. A prototype preamplifier with a noise level of 500 electrons (rms) has been designed,[13] and preliminary measurements[8] using a preproduction surface-mount-PCB version of the amplifier have demonstrated a charge division resolution of better than 1% of the 10 cm length of 7-μm-diam carbon sense fibers operating at an average total gas gain of 4×10^5.

Tests of a hybrid version of the amplifier, in which many of the discrete components have been gathered into a semicustom monolithic IC[(o)] are now well advanced, and the first production batch of amplifiers is expected shortly. We have also made considerable progress toward the integration of the CRID front end electronics with the Hybrid Analog Memory Unit (HAMU)[14]-based data acquisition system of the SLD.[15]

5. CONTROL AND MONITORING

Our test results indicate that our CRID design can operate efficiently enough to provide particle identification over the range needed at the SLD, but it is also necessary to develop a comprehensive and highly-automated monitor and control system to ensure long-term operation of the CRID at high efficiency.[2,16]

Of particular importance is the quality of the fluids entering the drift boxes and radiator enclosures, since the presence of electron- or UV-absorbing impurities can seriously degrade the performance of the detector. The UV transparency of all fluids entering and leaving the CRID will be monitored on a regular basis, as will the electron lifetime[8] in the gas entering and leaving the drift boxes. The composition of the drift and radiator gases will be periodically examined,[16] as will the levels of oxygen and water vapor following filter changeover.

Figure 9 is a compilation of UV transparency data for all the gases of current CRID interest. Of particular note is the improvement afforded by the use of filters[(p)] to remove oxygen and water vapor, which strongly absorb UV at wavelengths below 180 nm. The data for C_5F_{12} are derived from small samples: in the CRID gas system, C_5F_{12} will be recirculated through a large filter.

Due to the very high UV absorption coefficient of ethylene (C_2H_4: $\mu = 15530\ \mathrm{cm}^{-1}$ M^{-1} at $\lambda = 171$ nm),[8] we have seen a very wide variation in the UV transparency of commercial ethane (C_2H_6) samples. Processes which synthesize C_2H_6 from lower order hydrocarbon molecules (*e.g.,* Matheson "CP" grade: 99% purity) can leave

(*o*) Plessey Semiconductors, Scott's Valley, CA 95066.
(*p*) In this case, OXISORB.

sufficient C_2H_4 to seriously degrade the UV transparency. Although C_2H_4 can be removed during manufacture by expensive purification and quality control (*e.g.,* in Matheson "Research" grade C_2H_6: minimum purity 99.99%), less expensive sources of transparent C_2H_6 are those synthesized from higher order hydrocarbon molecules (*e.g.,* Liquid Carbonic "CP" grade [99%] followed by "first-stage"[19] purification).

6. CONCLUSION

The construction of the SLD barrel CRID is well advanced, and design studies for the endcap CRID have progressed sufficiently for detailed design to begin.

Acknowledgments

The assistance of the engineering and technical staffs at the collaborating institutions is gratefully acknowledged.

REFERENCES

1. SLD Design Report SLAC–273, UC–34D (May 1984).
2. G. Hallewell *et al.,* SLAC–PUB–4405; IEEE Trans. Nucl. Sci., **NS–35,** 398 (1988).
3. V. Ashford *et al.,* IEEE Trans. Nucl. Sci., **NS–34,** 499 (1987); SLAC–PUB–4118 (1986).
4. F. Bird *et al.,* SLAC–PUB–3790; IEEE Trans. Nucl Sci., **NS–33,** 261 (1986).
5. D. Aston *et al.,* SLAC–PUB–4785; submitted to the 1988 IEEE Nuclear Science Symposium, Orlando, FL (Nov. 1988).
6. J. Va'Vra *et al.,* SLAC–PUB–4432; IEEE Trans. Nucl. Sci., **NS–35,** 487 (1988).
7. M. Cavalli-Sforza, SLD CRID Internal Note No. 15 (1986).
8. (8) D. Aston *et al.,* "Development of the SLD CRID Single Electron Wire Detectors." Paper contributed to the 5th International Wire Chamber Conference, Vienna, Austria, Feb. 13–17, 1989.
9. R.T. Rewick *et al.,* SLAC–PUB–4415; Anal. Chem. **60,** 2095 (1988).
10. J. Va'Vra, SLD CRID Internal Note No. 36 (1988).
11. L. Mathys and M. Schneider, SLD CRID Internal Note No. 55 (1989).
12. P. Coyle *et al.,* SLAC–PUB–4403; submitted to the 1987 London Conference on Position-Sensitive Detectors; to be published in Nucl. Instr. and Meth.
13. E. Spencer *et al.,* SLAC–PUB–4404; IEEE Trans Nucl Sci, **NS–35,** 231 (1988).
14. J. Walker et al., SLAC–PUB–3503; IEEE Trans. Nucl. Sci., **NS–32,** 616 (1985).
15. SLD Collaboration (M. Breidenbach *et al.*), SLAC–PUB–4786; Submitted to the 1988 IEEE Nuclear Science Symposium, Orlando, FL (Nov. 1988).
16. G. Hallewell, SLD Internal Note 151 (Feb. 1986).

17. G. Hallewell *et al.,* SLAC–PUB–4122; Nucl. Instr.and Meth., **A264,** 219 (1988).

18. See, for example, T. W. Graham Solomons, "Fundamentals of Organic Chemistry,"(Wiley, 1982).

19. Proprietary Purification Technique Developed at Liquid Carbonic Laboratories, San Carlos, CA 94070.

FIGURE CAPTIONS

Figure 1. The SLD Čerenkov Ring Imaging Detector system.

(a) Principal components of the SLD CRID barrel and endcap systems.

(b) Engineering detail of the barrel CRID vessel and internal components: azimuthal arrangements at one end.

Figure 2. Measured surface resistivity of various epoxy adhesives vs. temperature.

Figure 3. Transmission measurements in quartz windows:

(a) Example of a quartz window sheet with a UV transparency considered acceptable for use in a drift box or liquid radiator tray; transmission exceeds 85% for (λ >175 nm).

(b) The effects of insufficient surface polish on the UV transparency; a rejected sheet.

(c) Example of poor transmission due to impurities in the bulk material; a rejected sheet.

Figure 4. The test station for the measurement of photoelectron drift distortion, electron lifetime and drift gas UV transparency.

Figure 5. The barrel CRID liquid C_6F_{14} radiator tray design.

(a) Deflection of a liquid C_6F_{14} radiator test tray (3.2-mm-thick glass window) under increasing applied hydrostatic pressure, showing eventual fracture. The vertical orientation has a baseline pressure of 0.06 Kg cm^{-2} from the liquid in the tray and feed lines, in addition to the applied pressure. In the horizontal orientation the contribution is 0.04 Kg cm^{-2}.

(b) Inset view of a barrel CRID liquid radiator tray (4 mm quartz window).

Figure 6. Characteristics of typical production mirrors.

(a) Typical RMS surface roughness measured in a 2 mm $\times$ 2 mm area scan upon a mirror substrate.

(b) Average UV reflectivity measured in a sample of 25 production mirrors for the barrel CRID: reflectivity exceeds 85% for ($\lambda > 170$ nm).

Figure 7. Measured pulse height spectrum in 80% C_2H_6/20% CO_2.

Figure 8. Possible blinding and focusing structure for the endcap CRID:

(a) Performance with the SLD magnetic field on.

(b) Performance with the SLD magnetic field off.

Figure 9. Compilation of UV transparency data for some gases of CRID interest, as measured in a 20 cm cell.

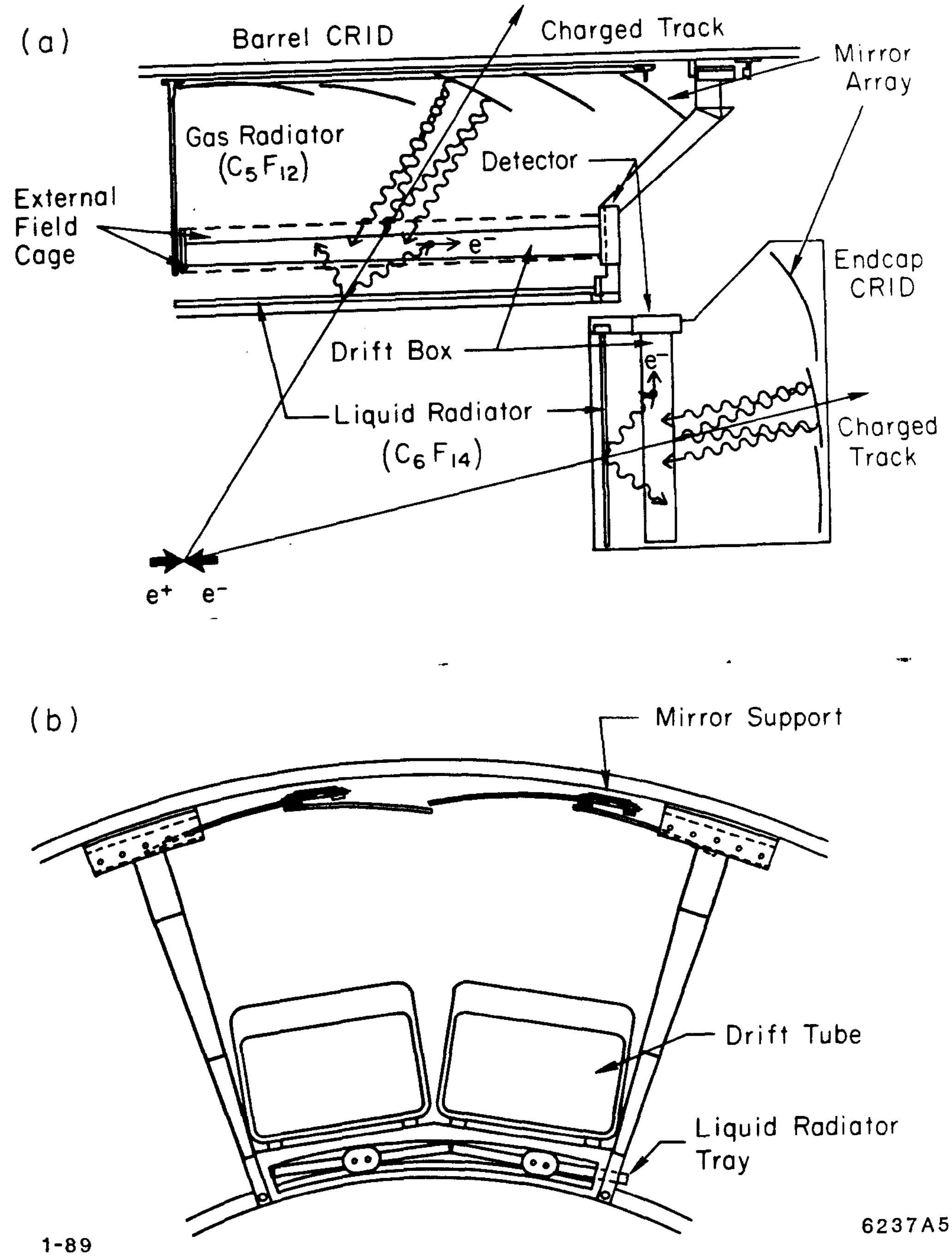

(a)
Barrel CRID
Charged Track
Mirror Array
Gas Radiator
(C_5F_{12})
Detector
External Field Cage
e⁻
Endcap CRID
Drift Box
e⁻
Liquid Radiator
(C_6F_{14})
Charged Track
e⁺ e⁻
(b)
Mirror Support
Drift Tube
Liquid Radiator Tray
1-89
6237A5

Fig. 1

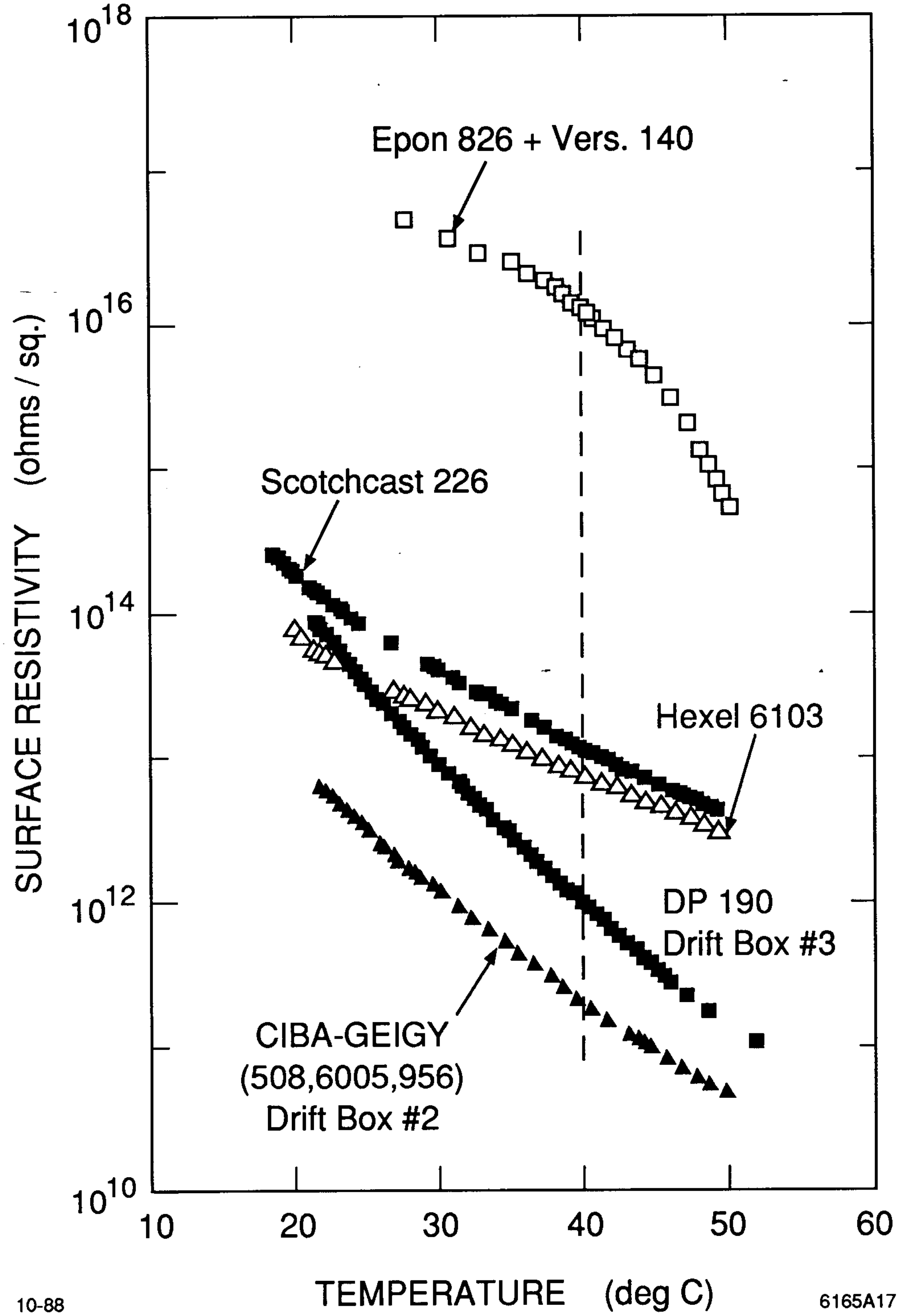

10^{18}
10^{16}
10^{14}
10^{12}
10^{10}
SURFACE RESISTIVITY (ohms / sq.)
Epon 826 + Vers. 140
Scotchcast 226
Hexel 6103
DP 190
Drift Box #3
CIBA-GEIGY
(508,6005,956)
Drift Box #2
10
20
30
40
50
60
TEMPERATURE (deg C)
10-88
6165A17

Fig. 2

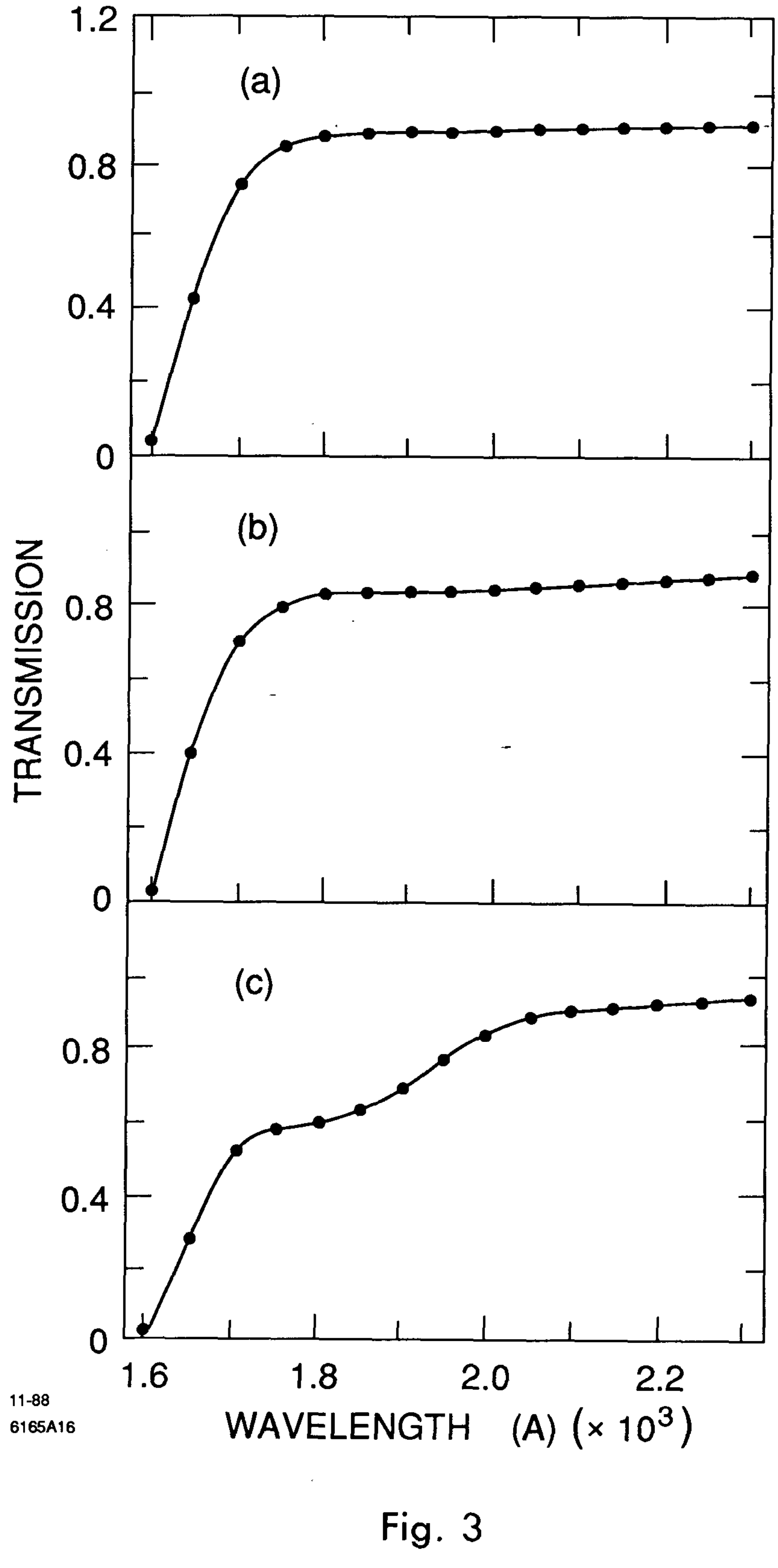
1.2
(a)
0.8
0.4
0
(b)
0.8
0.4
0
(c)
0.8
0.4
0
TRANSMISSION
1.6
1.8
2.0
2.2
WAVELENGTH (A) (× 10³)
11-88
6165A16

Fig. 3

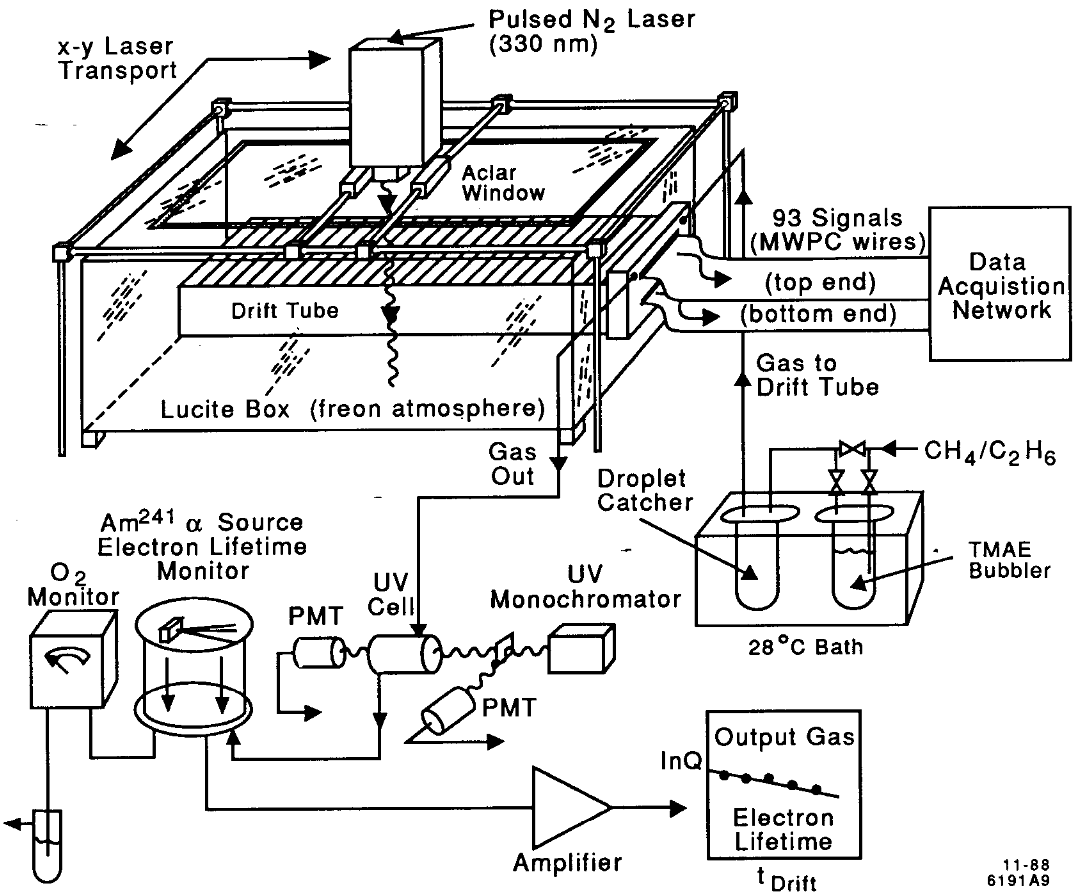
Pulsed N2 Laser
(330 nm)
x-y Laser
Transport
Aclar
Window
93 Signals
(MWPC wires)
Data
Acquistion
Network
(top end)
(bottom end)
Drift Tube
Gas to
Drift Tube
Lucite Box (freon atmosphere)
CH4/C2H6
Gas
Out
Droplet
Catcher
Am241 α Source
Electron Lifetime
Monitor
O2
Monitor
TMAE
Bubbler
UV
Cell
UV
Monochromator
PMT
PMT
28°C Bath
Output Gas
lnQ
Electron
Lifetime
t Drift
Amplifier
11-88
6191A9

Fig. 4

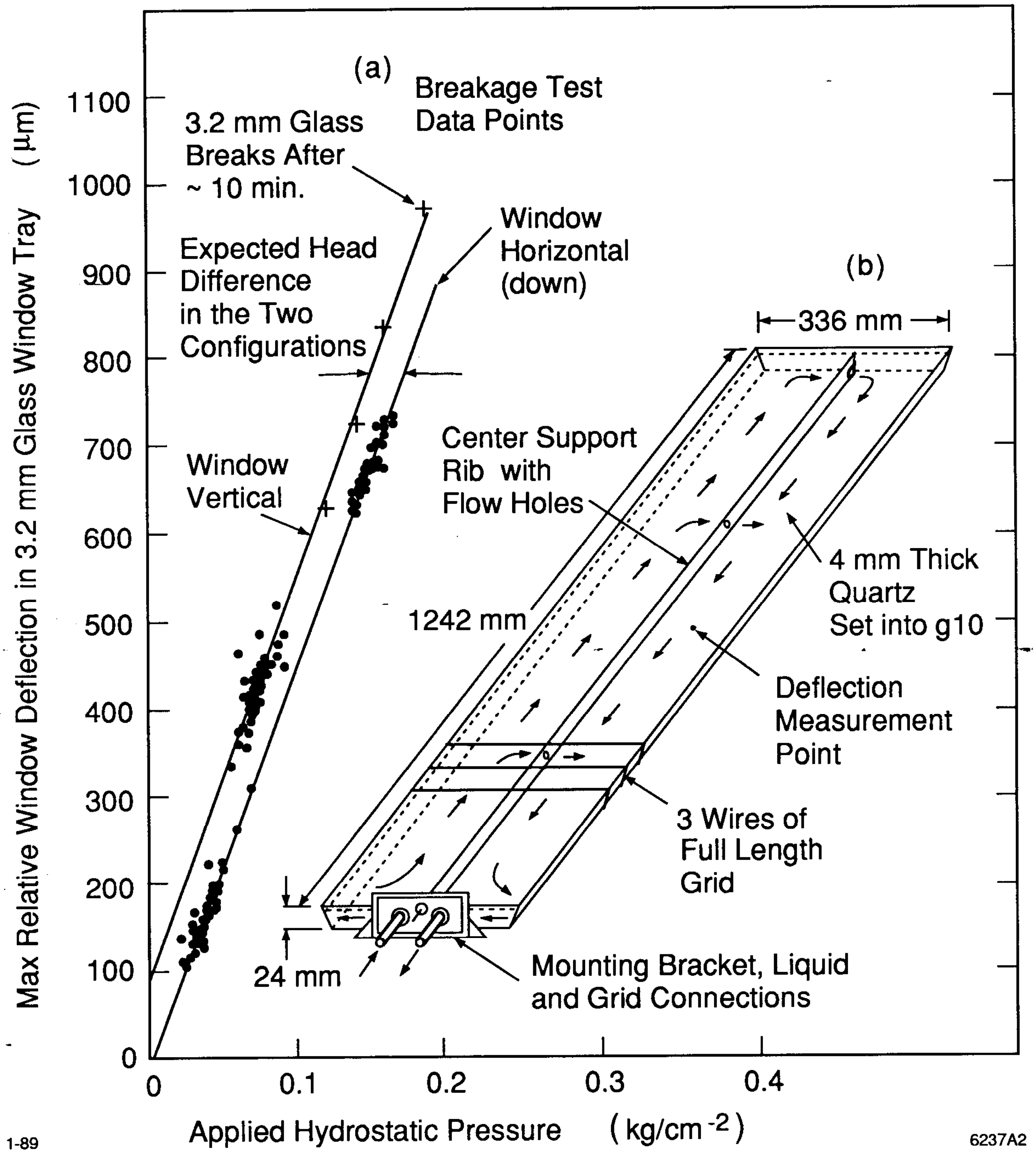

(a)
Breakage Test
Data Points
3.2 mm Glass
Breaks After
~ 10 min.
Window
Horizontal
(down)
Expected Head
Difference
in the Two
Configurations
Window
Vertical
Center Support
Rib with
Flow Holes
(b)
336 mm
4 mm Thick
Quartz
Set into g10
1242 mm
Deflection
Measurement
Point
3 Wires of
Full Length
Grid
24 mm
Mounting Bracket, Liquid
and Grid Connections
Max Relative Window Deflection in 3.2 mm Glass Window Tray (µm)
1100
1000
900
800
700
600
500
400
300
200
100
0
0
0.1
0.2
0.3
0.4
Applied Hydrostatic Pressure (kg/cm -2)
1-89
6237A2

Fig. 5

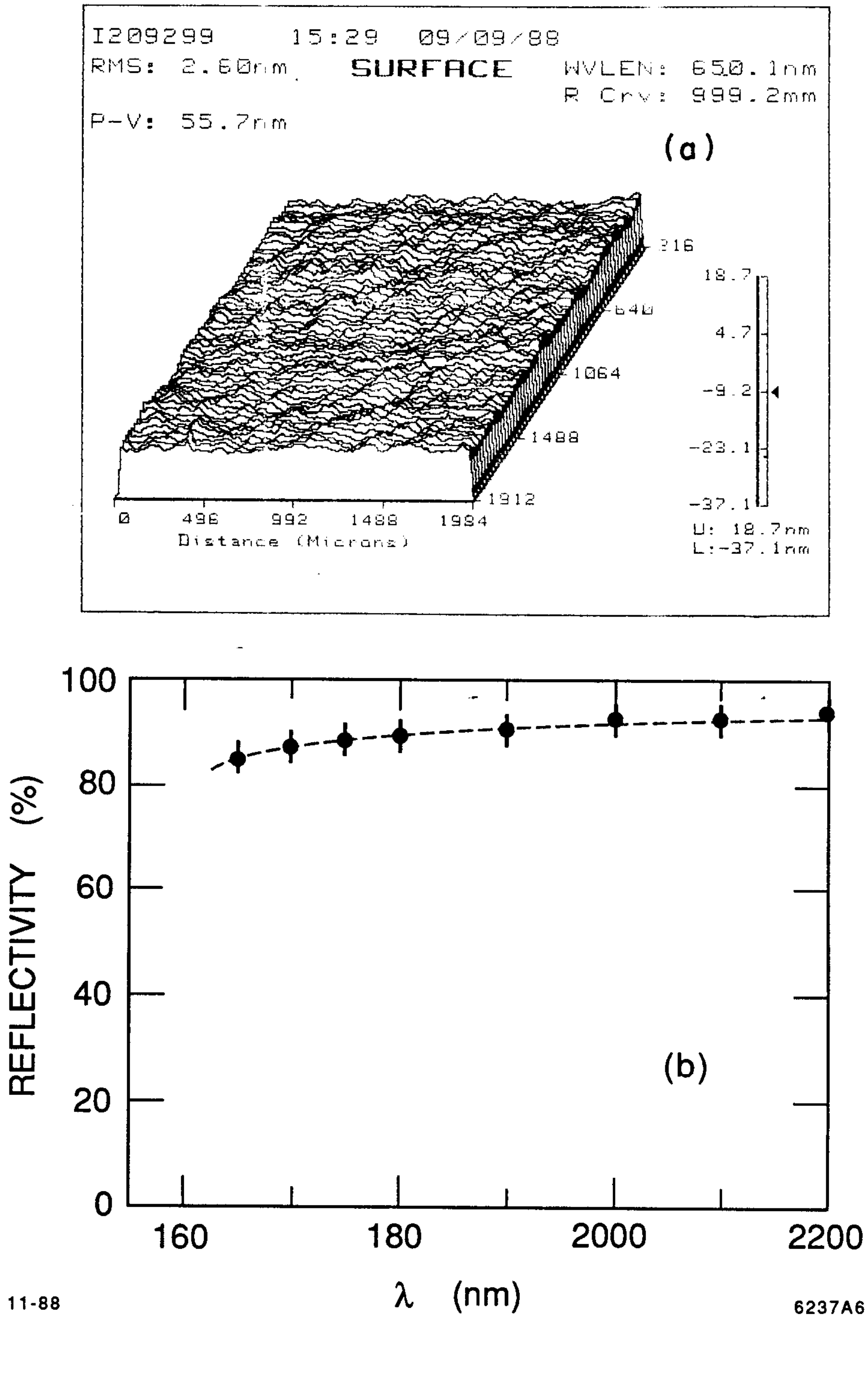
I209299 15:29 09/09/88
RMS: 2.60nm
SURFACE
WVLEN: 650.1nm
R Crv: 999.2mm
P-V: 55.7nm
(a)
216
640
1064
1488
1912
18.7
4.7
-9.2
-23.1
-37.1
0
496
992
1488
1984
Distance (Microns)
U: 18.7nm
L:-37.1nm
100
80
60
40
20
0
REFLECTIVITY (%)
(b)
160
180
2000
2200
λ (nm)
11-88
6237A6

Fig. 6

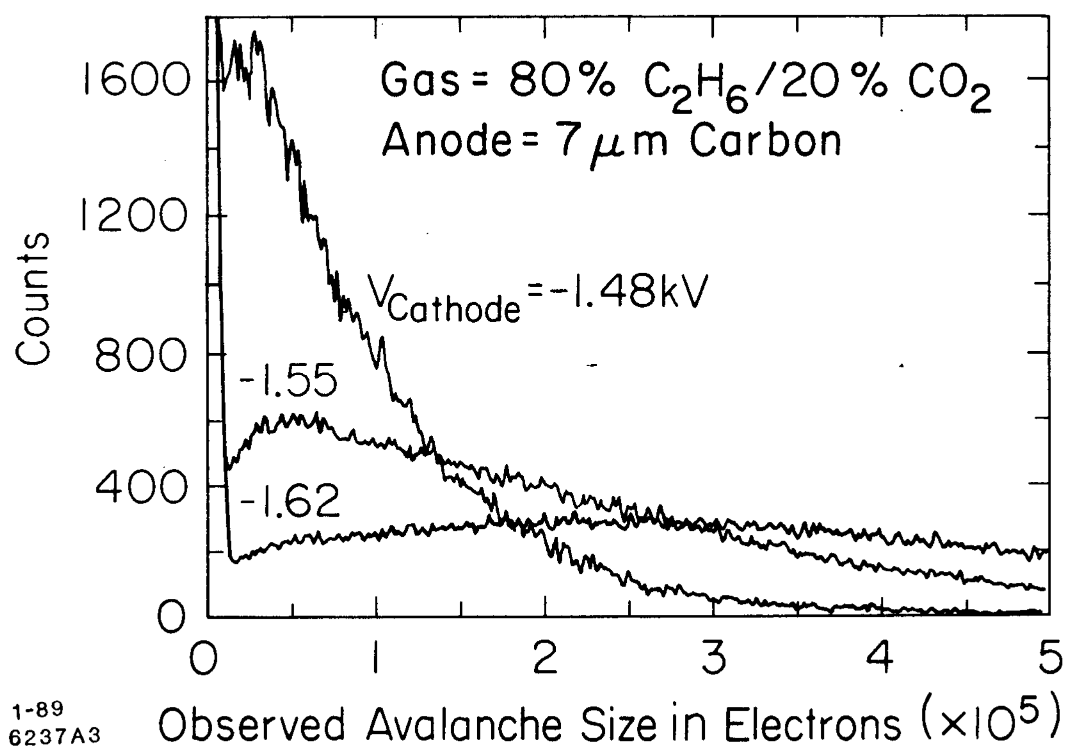
Gas = 80% C2H6/20% CO2
Anode = 7 μm Carbon
VCathode = -1.48kV
-1.55
-1.62
Counts
1600
1200
800
400
0
0
1
2
3
4
5
Observed Avalanche Size in Electrons (×10^5)
1-89
6237A3

Fig. 7

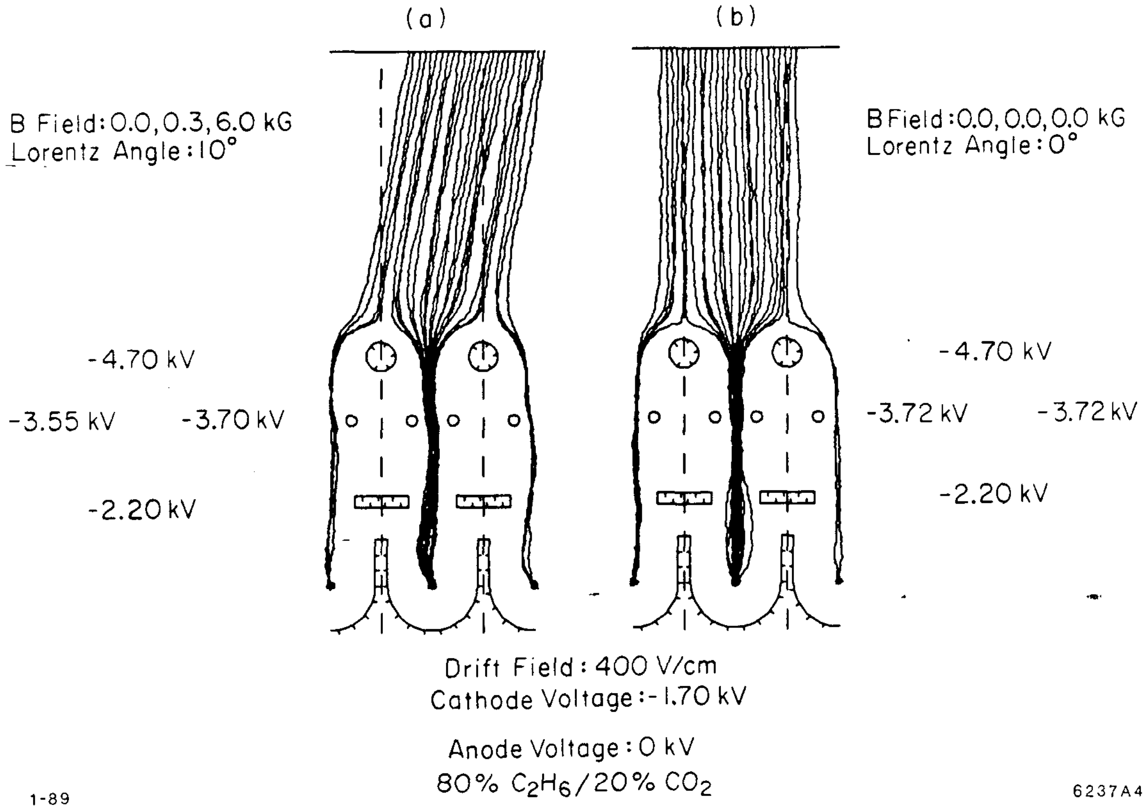
(a)
(b)
B Field: 0.0, 0.3, 6.0 kG
Lorentz Angle: 10°
B Field: 0.0, 0.0, 0.0 kG
Lorentz Angle: 0°
-4.70 kV
-3.55 kV
-3.70 kV
-2.20 kV
-4.70 kV
-3.72 kV
-3.72 kV
-2.20 kV
Drift Field: 400 V/cm
Cathode Voltage: -1.70 kV
Anode Voltage: 0 kV
80% C_2H_6/20% CO_2
1-89
6237A4

Fig. 8

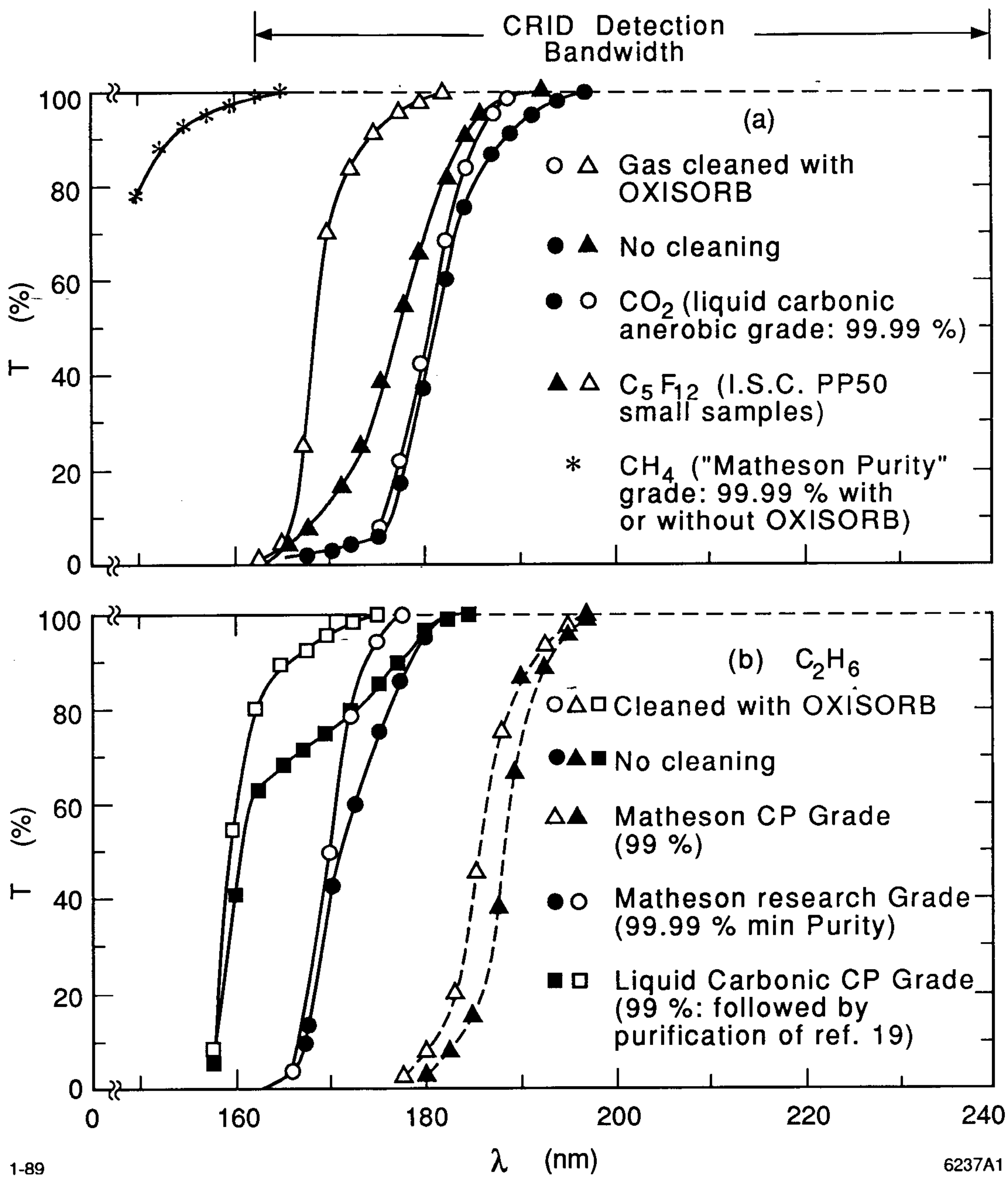
CRID Detection Bandwidth
T (%)
(a)
Gas cleaned with OXISORB
No cleaning
CO2 (liquid carbonic anerobic grade: 99.99 %)
C5F12 (I.S.C. PP50 small samples)
CH4 ("Matheson Purity" grade: 99.99 % with or without OXISORB)
(b) C2H6
Cleaned with OXISORB
No cleaning
Matheson CP Grade (99 %)
Matheson research Grade (99.99 % min Purity)
Liquid Carbonic CP Grade (99 %: followed by purification of ref. 19)
0
20
40
60
80
100
160
180
200
220
240
λ (nm)
1-89
6237A1

Fig. 9